IEEE Access
Multidisciplinary | Rapid Review | Open Access Journal

Received February 4, 2022, accepted March 1, 2022, date of publication March 8, 2022, date of current version March 21, 2022.

Digital Object Identifier 10.1109/ACCESS.2022.3157754

Design a New Time-Diversity System Using Orthogonal Mapping Matrix and Symbols Interleaving for Rayleigh Flat-Fading Channels

ASHRAF YAHIA HASSAN AND AHMED SAMI MOHAMMED
Benha Faculty of Engineering, Benha University, Banha 13511, Egypt
Corresponding author: Ashraf Yahia Hassan (ashraf.fahmy@bhit.bu.edu.eg)

ABSTRACT A time-diversity system is implemented in this work using a time-diversity encoder. The diversity encoder uses an orthogonal matrix to map vectors of N modulated symbols to vectors of N diversity symbols. Each modulated symbol is implicitly transmitted N times in N successive periods when the N diversity symbols are transmitted. No changes in the symbols' transmission rate occur due to the proposed time-diversity scheme. The diversity symbols are transmitted with the same transmission rate of modulated symbols in the systems with no signal diversity. The proposed system uses the same bandwidth of the system with no signal diversity too. In the receiver, the outputs of the matched filter are stored in a buffer of length N during the diversity period. After filling the buffer, its contents are multiplied with the inverse of the fading matrix. A diversity detector remaps the diversity symbols to the modulated symbols. It also combines the corresponding modulated symbols in one decision variable. The noise samples in the decision variables are uncorrelated. A maximum-likelihood (ML) detector and a linear detector are used as diversity detectors in this work. The performance of the proposed system achieves the same performance as the N diversity channels system with a unity-gain-combiner (UGC) receiver.

INDEX TERMS Time diversity, flat fading channels, orthogonal mapping, maximum likelihood detector, linear detector, unity-gain-combiner.

I. INTRODUCTION

In wireless communications, channel fading reduces the average signal-to-noise ratio (SNR) of the received signal. It disperses the transmitted symbols causing inter-symbol-interference (ISI). Signal diversity is used to improve signal quality in fading environments. It usually provides the receiver with different replicas of the transmitted symbols. The receiver gathers these replicas with a suitable signal-combining method to increase the received SNR [1], [2]. Signal diversity is usually done in space, time, and frequency. In space diversity, different transmitting and receiving antennas are used to send and receive the modulated symbols. Space diversity does not increase the bandwidth of the transmitted symbols or reduce the transmission rate of the modulated symbols. However, it produces interference between the received symbols [3], [4]. Space-time codes may be used in the transmitter of the space-diversity system to guarantee that the transmitted symbols are orthogonal in both spatial and time domains [5], [6]. The sphere detector and the QR-detector are used in the receiver to detect the modulated symbols and remove the interferences [7], [8]. Space-time codes increase the complexity of the transmitter and the receiver in space-diversity systems, but it keeps the spectrum efficiency of the system with no changes. In time diversity, the modulated symbols are transmitted more than once at different time epochs. The bandwidth of the transmitted symbols in time-diversity systems is the same as the bandwidth of the symbols transmitted in systems with no signal diversity. Time diversity improves the reliability of transmitting symbols in fading channels. However, the rate of the transmitted symbols is decreased, and this also decreases the spectrum efficiency of the time-diversity systems [9], [10]. In frequency diversity, the modulated symbols are transmitted more than once on different carrier frequencies at the same time. The transmission rate of the modulated symbols does not change in frequency-diversity systems; however, the symbols' bandwidth increases, and this decreases the bandwidth efficiency of the transmitted symbols [11], [12]. In spread-spectrum systems, spreading

The associate editor coordinating the review of this manuscript and approving it for publication was Ki-Hong Park.

codes may be used to get signal diversity. This type of diversity is called code diversity. Both code diversity and time diversity may be used together to get full signal diversity in fading environments with high Doppler frequency shift without changing the transmission rate of the modulated symbols [13]. In [14], a new method of signal diversity is proposed using orthogonal pulse shapes. This method achieves transmitting diversity of order two without using space-time codes.

In this paper, a new time-diversity system has been introduced to enhance the reliability of transmitting symbols in flat-fading channels. The proposed system does not have the disadvantage of the known time-diversity systems. The transmission rate of the modulated symbols does not change due to the used time-diversity scheme. Moreover, the bandwidth of the transmitted symbols in this work is the same as the bandwidth of the transmitted symbols in the systems with no signal diversity. Three factors give us the motivation to work on this system. The first is the power consumption in the transmitters of space-diversity systems. This work aims to reduce the power consumption in the transmitter by using one transmitting antenna with one deriving circuit. Using multiple antennas at the transmitter requires a separate RF driving circuit for each antenna. The power consumption of these circuits is not trivial [15]–[17]. Moreover, the transmitting antennas will experience cross-coupling, especially if they transmit signals with the same carrier frequency [18], [19]. The second factor is the complexity of the transmitter. In some systems such as wireless sensor networks, the complexity of the transmitter and the receiver are needed to be as small as possible [20], [21]. Additional hardware such as space-time encoders, space-time decoders, multiple transmitting antennas, multiple receiving antennas, and multiple driving circuits increase the complexity of the transmitter and the receiver. The third factor is that space-time codes fail to achieve full diversity and save the transmission rate to one symbol per channel use if the number of the transmitting antennas exceeds four antennas [22], [23].

The work in this paper is an extension of the work initiated in [24] and continued in [25]. The proposed work in this paper uses the same diversity encoder/decoder used in [25]. However, the proposed work in [25] uses frequency diversity instead of time diversity. The work in [25] achieved the required diversity gain by exploiting the random independent gains of the frequency-selective fading channel in the sub-channels of the orthogonal-frequency-division-multiplexing (OFDM) signal. The channel is assumed to be flat inside each OFDM subchannel, but it is frequency selective in the whole bandwidth of the OFDM signal. The bandwidth of the OFDM signal is N times the coherence bandwidth of the channel, where N is the number of the subchannels in the OFDM signal. The channel is assumed to be slowly fading in [25], where the period of the OFDM symbol is smaller than the coherence time of the channel. On the other hand, the current work is used with a single carrier system. The channel is assumed to be flat in the transmitted symbols' bandwidth. The current work achieves the required diversity gain by exploiting the random independent gains of the channel during the diversity period. The diversity period is the period through which the modulated symbol is transmitted more than one-time using different diversity symbols. The diversity period is equal to the coherence time of the channel multiplied by the required diversity order. Interleaving/deinterleaving blocks are used to disperse the diversity symbols from the same set of modulated symbols over different time slots with different channel gains inside the diversity period.

In the proposed time-diversity scheme, each modulated symbol is transmitted N times through N successive periods. To save the transmission rate of the modulated symbols, a diversity encoder is used to map vectors of N modulated symbols to vectors of N diversity symbols. The diversity symbols in the diversity vector are linear combinations of the input N modulated symbols to the diversity encoder. The diversity symbols are transmitted in N symbols periods, which represent the diversity interval of the modulated symbols. According to the used diversity scheme, ISI appears among the N modulated symbols in each symbol period. Here the interference is done on purpose. This ISI is completely removed from the received modulated symbols by using the diversity detectors. One transmitting antenna and one RF driving circuit are used to transmit the diversity symbols. The diversity order in the transmitter is equal to N. In the proposed diversity scheme, there is no relation between the transmission rate of the modulated symbols and the diversity order. The diversity order can be increased without affecting the transmission rate. Increasing the diversity order will merely increase the length of the diversity vector. This increases the latency of the transmitter and the number of interfering symbols in the diversity symbols.

This paper is organized as follows. Section 2 represents a revisit to time-diversity systems. In section 3, the methods used in this study are introduced. Section 4 represents the mathematical model of the modulated symbols and the proposed time-diversity symbols. It also shows the structure of the transmitter of the proposed system. Section 5 represents the received symbols model and the structure of the proposed received. A detailed analysis of the received symbols at each stage of the receiver is introduced in this section. Section 6 shows the maximum-likelihood (ML) diversity detector. The average probability of error in the received data from the proposed ML diversity detector is calculated for Rayleigh flat-fading channel. Section 7 shows the proposed linear-diversity detector. The performance of this detector is evaluated for Rayleigh flat-fading channel. The definition of the proposed unity-gain-combiner (UGC) with its mathematical model is introduced in section 7. A comparison between the UGC and the maximal-ratio-combiner (MRC) is also represented in this section. In section 8, the results and the discussions are represented. In this section, simulations of the proposed system are done using MATLAB. The results of a real-time implementation of the proposed system are

also introduced. The implementation is done using Xilinx Field Programmable Gate Array (FPGA) platform. The performance of the implemented system is compared with the performance results of the MATLAB simulations. Finally, the Conclusions are represented in section 9.

II. TIME DIVERSITY (REVISIT)

Time diversity is used to increase the power of the decision variables of the received symbols that were transmitted in a fading channel. In time diversity, the modulated symbols are transmitted in different time slots. The spacing between these time slots is bigger than or equal to the coherence time of the fading channel. The received symbols from the time diversity channels undergo independent fading gains. An MRC or a UGC are used to combine the corresponding received symbols from their different time slots in one decision variable. The power of the combined symbols is always bigger than the power of the received symbol from a single channel (one-time slot). The increase in the power of the received symbol depends on the time diversity order which is equal to the number of independent time slots used to transmit the modulated symbols.

Time diversity improves the power efficiency of the transmitted symbols in fading channels. However, it reduces the bandwidth efficiency of the transmitted symbols. The bandwidth efficiency is defined as the ratio between the transmission rate of the modulated symbols (R_s) and the bandwidth of the transmitted symbols (W) as shown in equation (1).

$$\eta_{BW} = \frac{R_s}{W} \tag{1}$$

In time-diversity system, the bandwidth of the transmitted symbols is the same as the bandwidth of the transmitted symbols in the systems with no signal diversity. The transmission rate of the time-diversity symbols (R_s^d) is equal to the symbol rate in the systems with no signal diversity divided by the time-diversity order (N) as shown in equation (2).

$$R_s^d = \frac{R_s}{N} \tag{2}$$

Therefore, the reduction factor in the bandwidth efficiency due to the time-diversity transmission is equal to the time-diversity order. This can be seen in [26] and in some systems that use time diversity [27]–[29]. The power efficiency in these systems has the most priority. However, the transmission rate and the bandwidth efficiency are reduced when the coherence time of the fading channel is small.

The poor bandwidth efficiency of the time diversity systems limits their usages in recent studies and recent systems. The space-diversity system can achieve moderate diversity gain without affecting bandwidth efficiency. Therefore, the recent studies concentrate on space-diversity applications such as the multiple-input-multiple-output (MIMO) applications in the 4G and 5G cellular networks [30], [31]. However, space-diversity systems cannot achieve high diversity gains without affecting the bandwidth efficiency. The reduction in the bandwidth efficiency in space-diversity systems is less than the reduction in the bandwidth efficiency in the time-diversity systems that achieve the same power gain. In the proposed work, high power gains can be achieved by time-diversity systems with the same bandwidth efficiency as the systems with no signal diversity.

TABLE 1. Comparison between the proposed time diversity and the conventional one.

	A proposed time-diversity system	A conventional time-diversity system
Time Diversity order	N	N
Symbol rate	R_s	R_s
Total symbol rate	R_s	$\frac{R_s}{N}$
Maximum Bandwidth	$2R_s$	$2R_s$
Minimum Bandwidth efficiency	50%	$\frac{50\%}{N}$
Maximum Average power gain	$10\log_{10}(N)$	$10\log_{10}(N)$

In this work, the bandwidth efficiency of the proposed time-diversity system is the same as the bandwidth efficiency of the system that uses the same transmission bandwidth and has the same transmission rate but with no signal diversity. In the proposed system, the average power of the combined received symbol is increased by the time-diversity order. For example, if the rate of the transmitted symbols in a communication system is 1M baud, and this system uses a raise-cosine shaping pulse with a roll-off factor equal to 0.5, the bandwidth of the transmitted symbols will be 1.5 MHz. The bandwidth efficiency of the system with no signal diversity is equal to 66.67%. If a conventional time-diversity is used with time-diversity order equal to 10, the average power of the received symbols will increase by 10 dB. However, 10 different time slots are used, and the total transmission rate of the time-diversity system is reduced to 100 K baud. In this case, the bandwidth efficiency of the time diversity system is equal to 6.67%. On the other hand, the symbol rate in the proposed time-diversity system does not change and the system achieves 8 dB increase in the power of the received symbols with a bandwidth efficiency of 66.67%. Table 1 shows a comparison between the proposed time-diversity system and the conventional time-diversity system.

III. METHOD

In the time-diversity system, different copies of the modulated symbol are received at different time slots with independent fading gains. The receiver combines these copies into a single decision variable to the baseband demodulator. The average SNR of this decision variable is bigger than the average SNR of individual copies of the modulated symbol. The period of the modulated symbol should be smaller than or equal to the coherence time of the channel to have independent fading gains. In the conventional time-diversity systems, a modulated symbol is transmitted in N

consecutive time slots. This reduces the transmission rate of the modulated symbols. However, in the proposed system, time diversity is achieved without changing the transmission rate. A diversity encoder is used to map N modulated symbols to N diversity symbols using an orthogonal mapping matrix. The diversity symbols are transmitted with the same transmission rate as the modulated symbols in the systems with no signal diversity. In this way, the modulated symbol is transmitted in N consecutive periods without affecting the transmission rate. If the symbol period of the modulated symbol is T_s, the diversity interval in the proposed system will be equal to $N \times T_s$.

In the receiver, one antenna is used to receive the transmitted signal. The received signal passes through one matched filter, which is matched to the shaping pulse of the received diversity symbols. The outputs of the matched filter are stored in a buffer of length N during the diversity period of the modulated symbol. After the buffer has been filled, the buffered symbols are multiplied with the inverse of the channel matrix to compensate for the fading effect. The output vector of the channel compensation process represents the observation vector to the diversity detector. The noise samples in this observation vector are uncorrelated. This fact plays an important role in our proposed system. A diversity detector uses the observation vector to remap the received symbols from the space of diversity symbols to the space of modulated symbols. It also combines the corresponding modulated symbols into a single decision variable. Two different diversity detectors are introduced in this work. The first diversity detector is the ML detector, which is based on the ML detection theory. The second diversity detector is the linear decorrelator detector. The decorrelator detector multiplies the observation vector with the inverse of the mapping matrix used in the transmitter. The diversity detectors exploit the existence of the diversity symbols to achieve the required diversity gain and to improve the estimations of the modulated symbols.

In this work, different methodologies are used to study the proposed time-diversity scheme and the diversity detectors. The first methodology is a mathematical study. In this study, a mathematical model of the received time-diversity symbol is introduced based on the used time diversity encoder in the transmitter. The mathematical models of the symbols at each stage in the receiver are also introduced. These mathematical models show how the SNR of the decision variable is increased with the proposed time-diversity system. The proposed combining method introduce by the mathematical model is the UGC and it is a sub-optimum method if it is compared with the optimum MRC. The second methodology is the simulation of the proposed time-diversity system with two different diversity detectors. The first diversity detector is based on the ML criterion. The process of diversity decoding and the process of symbols combining are done implicitly inside the ML detector. The second diversity detector is the decorrelator detector, which is based on the zero-forcing criterion. The decorrelator detector extracts the modulated symbols from the observation vector and combines the corresponding symbols in one decision variable. Simulations are done using MATLAB. M-files scripts are written according to the mathematical models of the symbols derived from the mathematical study. The simulations are done at different conditions and situations to evaluate the performance of the proposed time-diversity receiver with the proposed diversity detectors. Finally, real-time transmitter and receiver are implemented, and real-time measurements are obtained for the performance of the proposed time-diversity system. The results from the used three methodologies are compared with each other and according to this comparison, the final contribution is deduced.

During the second and third methodologies, the performance of the proposed system is measured using two different criteria. The first criterion is the bit-error-rate (BER) criterion. The average BER is calculated at the output of two different receivers with an ML diversity detector and a decorrelator diversity detector. The second criterion is the average noise power at the output of the diversity detectors. The average noise power is measured at the output of the ML diversity detector, and it is compared with the measured average noise power at the output of the decorrelator diversity detector. More details on the testing and the measurements are represented in the section of the results and discussions.

IV. THE PROPOSED MODEL OF A TIME-DIVERSITY SYMBOL

In the proposed time-diversity system, the symbols from the baseband modulator are arranged in vectors of N modulated symbols. A new block called a diversity encoder maps these vectors to vectors of N diversity symbols in an N-dimensions space using a Hadamard orthogonal matrix of order N. The new vectors of the diversity symbols are called diversity vectors. Equation (3) shows the diversity symbol x_{km}, which is the m^{th} diversity symbol in the k^{th} diversity vector at the output of the diversity encoder.

$$x_{km} = \sum_{n=1}^{N} s_{mn}.d_{kn} \quad 1 \le m \le N. \tag{3}$$

d_{kn} is the n^{th} modulated symbol in the k^{th} input vector to the diversity encoder. s_{mn} is the element in the m^{th} row and n^{th} column of the Hadamard orthogonal matrix of order N. s_{mn} takes values from the set $\{-1, +1\}$. It represents the mapping coefficient of the n^{th} modulated symbol to the m^{th} diversity symbol. Equations (4.a) and (4.b) show the relation between the k^{th} input and output vectors of the diversity encoder.

$$\mathbf{x_k} = \mathbf{S}.\mathbf{d_k} \tag{4.a}$$

$$\begin{bmatrix} x_{k1} \\ x_{k2} \\ \vdots \\ x_{kN} \end{bmatrix} = \begin{bmatrix} s_{11} & s_{12} & \cdots & s_{1N} \\ s_{21} & s_{22} & \cdots & s_{2N} \\ \vdots & \vdots & \ddots & \vdots \\ s_{N1} & s_{N2} & \cdots & s_{NN} \end{bmatrix} \begin{bmatrix} d_{k1} \\ d_{k2} \\ \vdots \\ d_{kN} \end{bmatrix} \tag{4.b}$$

The matrix $\mathbf{S}$ is a Hadamard orthogonal matrix of order N. The matrix $\mathbf{S}$ is selected to be an orthogonal matrix

to have optimum detection in the receiver as will be shown in section 6. From equation (3), each diversity symbol in the diversity vector implicitly carries information about the N modulated symbols in the input vector to the diversity encoder. The diversity symbols in the diversity vector are transmitted through N consecutive symbol periods. Therefore, each modulated symbol in vector $\mathbf{d}_k$ is indirectly transmitted N times through N consecutive periods. These periods represent the diversity periods of the modulated symbols. The proposed time-diversity system achieves a transmission rate of one symbol per channel use. The diversity encoder introduces intentional interference among the modulated symbols. The receiver should have the ability to remove this intentional interference. This is the cost, which should be paid to achieve the proposed time-diversity gain.

From the perspective of the fading channel, the diversity interval of the modulated symbols should be equal to $N \times \Delta t$ to have N independent fading gains in the received diversity symbols. The time Δt is the coherence time of the fading channel and it is equal to the reciprocal of the Doppler frequency shift occurred in the channel. So far, it is assumed that the modulated symbol period is equal to the coherence time of the channel ($T_s = \Delta t$). But what will happen if the coherence time of the channel is smaller than or greater than the modulated symbol period?

The previous question has two answers depending on whether the channel model is slow fading or fast fading. In our system design, we will use the slow fading channel model because the proposed system should support high data rate transmission. In this case, the modulated symbol period is smaller than the coherence time of the fading channel ($T_s < \Delta t$). In slow fading channel, the fading gain is almost fixed during D modulated symbols. The value of D is the floor of dividing the channel coherence time and the modulated symbol period as shown in equation (5).

$$D = \left\lfloor \frac{\Delta t}{T_s} \right\rfloor \tag{5}$$

Therefore, the N diversity symbols in the diversity vector must be transmitted in N time slots that are spaced by D symbols period to have N independent fading gains. This changes the target transmission rate of the modulated symbols, and the system will lose its benefit, which is achieving high diversity gain without changing the transmission rate of the modulated symbols and without changing the transmission bandwidth. To solve this problem, symbols interleaving is used after the diversity encoder. The symbols interleaving has a depth of N diversity symbols and a width of D diversity vectors as shown in figure 1.

The diversity symbols are stored in the interleaving memory column-wise and they are transmitted row-wise. For the k^{th} diversity vector, the first diversity symbol is transmitted and after $D-1$ symbols periods the second diversity symbol from the same vector is transmitted, and so on till all diversity symbols stored in the interleaving memory are transmitted. During the $D-1$ symbols periods

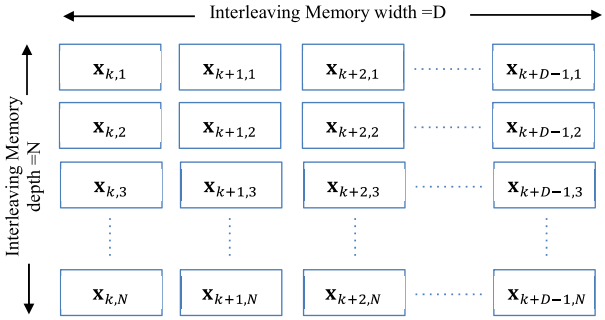

FIGURE 1. The diversity symbols interleaving.

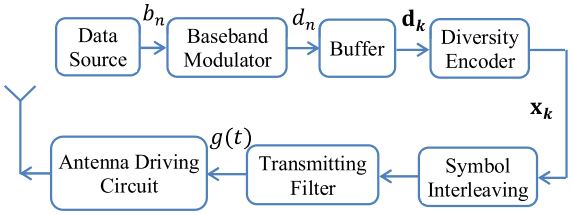

FIGURE 2. The transmitter of the proposed time-space diversity system.

after transmitting the first diversity symbol in the k^{th} diversity vector, the first diversity symbols in the consecutive $D-1$ diversity vectors are transmitted. The symbols interleaving increases the latency of the transmitter, but it saves the transmission rate of the modulated symbols as that of the systems with no time diversity. Figure (2) shows the block diagram of the transmitter of the proposed time-diversity system.

The n^{th} binary symbol b_n from the data source is modulated to a complex QAM symbol d_n using a baseband modulator. A buffer is used to store N modulated symbols from the baseband modulator through N consecutive symbols periods. The diversity encoder maps the stored N modulated symbols in the k^{th} buffered vector to N diversity symbols using the Hadamard orthogonal matrix S as shown in equation (4.a). Symbols interleaving of N symbols depth and D vectors width is used to interleave the $N \times D$ diversity symbols of the D diversity vectors. The latency of the transmitter of the proposed time-diversity system is $N \times (D+1)$ symbols periods. In the slow fading model, the diversity period is equal to $(N \times T_s)$. This is the period required to have N independent fading gains for one diversity vector (N diversity symbols). The diversity period for the slow fading model is not continuous. It consists of N time slots of width T_s each. The spacing between these time slots is equal to $(D \times T_s)$. The diversity symbols from the symbols interleaving are sent to the transmitting filter. The transmitting filter output $g(t)$ is sent to the driving circuit of the antenna. The impulse response of the transmitting filter represents the shaping pulse of the transmitted diversity symbols. Orthogonal shaping pulses may be used to duplicate the transmission rate of the diversity symbol [32]. But a conventional shaping pulse will be used in the following analysis for simplicity. The transmitted diversity symbol is normalized to have unit

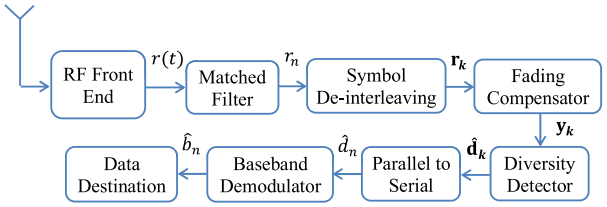

FIGURE 3. The receiver of the proposed time-space diversity system.

energy during the symbol period T_s. The driving circuit of the antenna consists of an RF mixer, a power amplifier, and a matching circuit. The RF mixer is used to transfer the baseband diversity symbols to the passband symbols at a certain carrier frequency f_c. Since the proposed diversity encoder produces N diversity symbols corresponding to N modulated symbols and sends these symbols through N symbols periods, the symbols transmission rate is one modulated symbol per channel use.

V. THE STRUCTURE OF THE PROPOSED RECEIVE

In this work, the Rayleigh flat fading channel is used to model the channel from the proposed transmitter to the proposed receiver. The fading channel affects the magnitude and the phase of the transmitted symbol. It is assumed that the complex fading gain is constant during D symbol periods and it changes randomly every $D \times T_s$ second. The transmitted symbol is also corrupted with additive white Gaussian noise. Figure (3) shows the receiver of the proposed diversity system.

In the proposed receiver, one antenna is used to receive the symbols from the fading channel. The first stage in the receiver is the RF front end. It consists of the low noise amplifier and the RF down converter. A matched filter is used to process the baseband signal after the RF front-end. The matched filter must be matched to the shaping pulse of the received symbols to have maximum SNR at its output. The shape of the received symbols $h(t)$ is equal to the convolution between the shaping pulse of the transmitted symbols $g(t)$ and the impulse response of the fading channel $c(t)$ as shown in equation (6).

$$h(t) = g(t) \star c(t) \tag{6}$$

According to the assumption of flat fading, the channel impulse response is approximately an impulse function but with complex Gaussian random weight. Equation (7) shows the n^{th} output of the matched filter in the n^{th} symbol period.

$$r_n = \int_0^{T_s} r(\tau)\, h^*(\tau - nT_s)\, .d\tau = \alpha_n e^{j\phi_n} x_n + w_n \tag{7}$$

α_n is a Rayleigh random variable. ϕ_n is a uniform random variable. α_n and ϕ_n represent the fading gain and phase shift at the n^{th} symbol period, respectively. x_n is the n^{th} diversity symbol. w_n is the noise random variable. It is the output of the matched filter due to an input sample function $w(t)$ of a white Gaussian noise process W(t). The noise sample function $w(t)$ has a zero mean and $\sigma_w^2\delta(t)$ auto-correlation function. Equation (8) shows the noise sample at the output of the matched filter at the n^{th} symbol period.

$$w_n = \int_0^{T_s} w(\tau)\, .h^*(\tau - nT_s)\, .d\tau \tag{8}$$

The received diversity symbols from the matched filter are delivered to the symbols deinterleaving, which performs the inverse operation of the symbols interleaving in the transmitter. The symbols deinterleaving saves the received diversity symbols in its memory row-wise. The output diversity vectors are read from the deinterleaving memory column-wise. The deinterleaving memory width is equal to D diversity vectors and its depth is equal to N diversity symbols. The vector $\mathbf{r_k}$ in equation (9.a) is the output vector from the deinterleaving memory. It represents the k^{th} received diversity vector. It is corresponding to the diversity vector $\mathbf{x_k}$ at the output of the diversity encoder in the transmitter. The n^{th} element in the k^{th} received diversity vector $\mathbf{r_k}$ is shown in equation (9.c).

$$\mathbf{r_k} = \mathbf{A_k}.\mathbf{x_k} + \mathbf{w_k} \tag{9.a}$$

$$\mathbf{A_k} = \begin{bmatrix} \alpha_{k1}e^{j\phi_{k1}} & 0 & \dots & 0 \\ 0 & \alpha_{k2}e^{j\phi_{k2}} & \dots & 0 \\ \vdots & \vdots & \ddots & \vdots \\ 0 & 0 & \dots & \alpha_{kN}e^{j\phi_{kN}} \end{bmatrix} \tag{9.b}$$

$$r_{kn} = \alpha_{kn}e^{j\phi_{kn}}x_{kn} + w_{kn} \tag{9.c}$$

The diagonal matrix $\mathbf{A_k}$ is the channel matrix that affects the k^{th} diversity vector $\mathbf{x_k}$. The diagonal elements of $\mathbf{A_k}$ represent the complex fading gains of the N diversity symbols in the k^{th} received diversity vector $\mathbf{r_k}$. These gains are independent since the time-space between the received diversity symbols in $\mathbf{r_k}$ is equal to the coherence time ($\Delta t = D \times T_s$ second).

The noise random variables w_{kn} and w_{km} in the k^{th} received diversity vector $\mathbf{r_k}$ are uncorrelated. They are produced from two different sample functions $w_{kn}(t)$ and $w_{km}(t)$ of a white Gaussian noise process W(t) at the n^{th} and the m^{th} coherence periods. Equations (10.a) and (10.b) show the correlation between the noise random variables in the noise vector $\mathbf{w_k}$.

$$\begin{aligned} E\left[w_{kn}.w_{kn}^*\right] &= E\left[\int_0^{T_s} w_{kn}(t_1)\, .h^*(t_1 - nT_s)\, .dt_1 \right. \\ &\quad \left. \int_0^{T_s} w_{kn}^*(t_2)\, .h(t_2 - nT_s)\, .dt_2\right] \\ &= \int_0^{T_s}\int_0^{T_s} E\left[w_{kn}(t_1)\, w_{kn}^*(t_2)\right].h^*(t_1 - nT_s) \\ &\quad .h(t_2 - nT_s)\, .dt_1.dt_2 \\ &= \sigma_w^2 \end{aligned} \tag{10.a}$$

$$\begin{aligned} E\left[w_{kn}.w_{km}^*\right] &= E\left[\int_0^{T_s} w_{kn}(t_1)\, .h^*(t_1 - nT_s)\, .dt_1 \right. \\ &\quad \left. .\int_0^{T_s} w_{km}^*(t_2)\, .h(t_2 - mT_s)\, .dt_2\right] \\ &= \int_0^{T_s}\int_0^{T_s} E\left[w_{kn}(t_1)\, w_{km}^*(t_2)\right].h^*(t_1 - nT_s) \\ &\quad .h(t_2 - mT_s)\, .dt_1.dt_2 \\ &= 0 \end{aligned} \tag{10.b}$$

The covariance matrix of the noise vector $\mathbf{w_k}$ in equation (9.a) is:

$$\boldsymbol{cov}\left[\mathbf{w_k}, \mathbf{w_k}\right] = \boldsymbol{E}\left[\mathbf{w_k}.\mathbf{w_k^H}\right] = \sigma_w^2\mathbf{I} \tag{11}$$

It is assumed that the channel status information (CSI) is known at the receiver. Pilot signals or channel estimation algorithms may be used to feed the receiver with this information. The estimation error of CSI affects the receiver performance. However, in this work it is assumed that the channel gains are estimated perfectly, and they are provided to the receiver with no estimation error. The estimation of CSI and the effect of the estimation error are out of the scope of this paper. The CSI estimation will be treated in a separate future work.

To compensate for the fading effect of the channel, the received diversity vector in equation (9.*a*) is multiplied with the inverse of the channel matrix $\mathbf{A_k}$. The output vector $\mathbf{y_k}$ of the fading-compensation process is shown in equation (12).

$$\mathbf{y_k} = \mathbf{A_k^{-1}}.\mathbf{r_k} = \mathbf{x_k} + \mathbf{A_k^{-1}}.\mathbf{w_k} \tag{12}$$

The m^{th} element in the output diversity vector $\mathbf{y_k}$ of the fading compensation process is:

$$y_{km} = \sum\nolimits_{n=1}^{N} s_{mn}.d_{kn} + \frac{e^{-j\phi_{kn}}.w_{km}}{\alpha_{kn}} \tag{13}$$

The noise components in the compensated diversity vector $\mathbf{y_k}$ are also independent because the covariance matrix of the noise vector $\left(\mathbf{A_k^{-1}}.\mathbf{w_k}\right)$ is diagonal, and it is equal to $\sigma_w^2\mathbf{A_k^{-2}}$. The diversity symbols in the compensated diversity vector $\mathbf{y_k}$ have unity gains after fading compensation. This is why the proposed combining method is called a unity-gain combiner.

After channel compensation process, a diversity detector is used to estimate the k^{th} vector of modulated symbols. In this proposal, the function of the diversity detector is performed using a multi-symbol detector. The multi-symbol detector removes the interferences among the modulated symbols in the compensated diversity vector in equation (12). It also combines the corresponding modulated symbols from the N diversity symbols in one decision variable to the baseband demodulator.

Two multi-symbol detectors are proposed to do the function of the diversity detector. The first detector is the ML multi-symbol detector. It removes the interference between the diversity symbols and estimates the vector of the modulated symbols, simultaneously. The ML multi-symbol detector is designed to implicitly combine the corresponding modulated symbols from the compensated diversity vector. However, if the ML detector is designed to estimate the diversity symbols, a separate diversity decoder will be required to perform the combining process. In this work, the ML multi-symbol detector is designed according to the first approach. The second proposed detector is the decorrelator detector. It is a linear detector that applies the inverse mapping process directly to the compensated diversity vector. It also combines the corresponding modulated symbols from the N received diversity symbols in the compensated diversity vector and calculates their average. The output vector from the decorrelator detector is the decision vector to the baseband demodulator. The elements of the decision vector are the estimations of the modulated symbols.

VI. MAXIMUM LIKELIHOOD MULTI-SYMBOLS DETECTOR

Multi-symbols detectors are the detectors, which extract the interfering symbols from the received signal. They remove or minimize the interference among these symbols according to the used criterion of operation. The multi-symbol detectors are analogous to spatial detectors in spatial-multiplexing MIMO (SM-MIMO) systems. It is also similar to the multiuser detectors in multiuser systems [33]. However, the detected symbols by the multi-symbols' detectors belong to the same user instead of multiple users.

The vector $\mathbf{y_k}$ in equation (12) represents the observation vector to the ML multi-symbols detector in N-dimensions observation space. The ML multi-symbols detector estimates the vector of the modulated symbols from this observation vector. The detector chooses the modulated vector, whose mapping by Hadamard orthogonal matrix $\mathbf{S}$ has the shortest distance with the observation vector. This is equivalent to choosing the vector of the modulated symbols $\hat{\mathbf{d}}_\mathbf{k}$, which maximizes the posterior probability $p(\mathbf{d_k}/\mathbf{y_k})$ of the modulated symbols vector given the observation vector $\mathbf{y_k}$.

$$\hat{\mathbf{d}}_\mathbf{k} = arg\left[\max_{\mathbf{d_l}}\left(p\left(\mathbf{d_l}/\mathbf{y_k}\right)\right)\right] \tag{14}$$

The same vector maximizes the likelihood function $p(\mathbf{y_k}/\mathbf{d_k})$ because the vectors of the modulated symbols are equiprobable. Therefore, the optimum choice of the vector of the modulated symbols is the vector $\hat{\mathbf{d}}_\mathbf{k}$, which maximizes the likelihood function $p(\mathbf{y_k}/\mathbf{d_k})$ as shown in equation (15).

$$\hat{\mathbf{d}}_\mathbf{k} = arg\left[\max_{\mathbf{d_l}}\left(p\left(\mathbf{y_k}/\mathbf{d_l}\right)\right)\right] \tag{15}$$

The covariance matrix of the noise in the observation vector $\mathbf{y_k}$ is:

$$\boldsymbol{cov}\left[\mathbf{A_k^{-1}}.\mathbf{w_k}\right] = \sigma_w^2\left|\mathbf{A_k}\right|^{-2} \tag{16}$$

Since the channel matrix $|\mathbf{A_k}|^{-2}$ is diagonal, the noise samples in vector $\left(\mathbf{A_k^{-1}}.\mathbf{w_k}\right)$ are uncorrelated. Therefore, the likelihood function $p(\mathbf{y_k}/\mathbf{d_l})$ of the l^{th} received vector is defined as:

$$p\left(\mathbf{y_k}/\mathbf{d_l}\right) = \frac{1}{(2\pi)^N\prod_{n=1}^{N}\alpha_{kn}^{-2}\sigma_w^2} \times exp\left(\frac{-\left(\mathbf{y_k}-\mathbf{S}.\mathbf{d_l}\right)^H\left|\mathbf{A_k}\right|^2\left(\mathbf{y_k}-\mathbf{S}.\mathbf{d_l}\right)}{2\sigma_w^2}\right) \tag{17}$$

The solution of equation (15) is the vector $\hat{\mathbf{d}}_k$, which maximizes the sufficient statistic $L(\mathbf{y}_k)$.

$$\begin{aligned}\hat{\mathbf{d}}_k &= arg\left[\max_{\mathbf{d}_l}\left(L\left(\mathbf{y}_k\right)\right)\right] \\ &= arg\left[\max_{\mathbf{d}_l}\left(2Re\left(\mathbf{d}_l^H.\mathbf{S}^H\left|\mathbf{A}_k\right|^2.\mathbf{y}_k\right)\right.\right. \\ &\quad \left.\left.-\mathbf{d}_l^H.\mathbf{S}^H\left|\mathbf{A}_k\right|^2\mathbf{S}.\mathbf{d}_l\right)\right] \end{aligned} \tag{18}$$

The elements of $\hat{\mathbf{d}}_k$ are the estimations of the modulated symbols in the k^{th} modulated period. The ML multi-symbol detector implicitly applies the algorithm of the diversity decoder. This appears in equation (18), where the orthogonal mapping matrix $\mathbf{S}$ is used in the calculations of the sufficient statistic $L(\mathbf{y}_k)$.

Equation (19) represents the conditional probability of error in the n^{th} symbol of vector $\hat{\mathbf{d}}_k$ when the M-QAM scheme is used in the proposed system [34], [35]. It is assumed that the fading gain α_{kn} is known.

$$p_e\left(\hat{d}_{kn}/\alpha_{kn}\right) = \left(1-\frac{1}{\sqrt{M}}\right)\text{erfc}\left(\sqrt{\frac{3\alpha_{kn}^2E_s}{2\left(M-1\right)\sigma_w^2}}\right) \tag{19}$$

E_s is the average energy of the modulated M-QAM symbols. According to the detection rule of the k^{th} vector of modulated symbols $\hat{\mathbf{d}}_k$ in equation (18), the conditional probability of error in estimating the k^{th} symbols vector $\hat{\mathbf{d}}_k$, given the fading gain matrix $|\mathbf{A}_k|$, is:

$$\begin{aligned}p_e\left(\hat{\mathbf{d}}_k/\left|\mathbf{A}_k\right|\right) &= \left(1-\frac{1}{\sqrt{M}}\right)\text{erfc} \\ &\quad\times\left(\sqrt{\frac{3\mathbf{d}_k^H\mathbf{S}^H.\mathbf{S}\mathbf{d}_k}{2\left(M-1\right)\sigma_w^2.tr(|\mathbf{A}_k|^{-2})}}\right)\end{aligned} \tag{20}$$

The term $\left(\mathbf{d}_k^H\mathbf{S}^H\mathbf{S}\mathbf{d}_k\right)$ represents the energy of the k^{th} symbols vector after combining the corresponding modulated symbols in the decision vector. It is equal to $N^2\times E_s$. The term $\sigma_w^2.tr(|\mathbf{A}_k|^{-2})$ represents the noise power in the observation vector $\mathbf{y}_k$. After some mathematical manipulations on equation (20), the conditional probability of error in demodulated vector $\hat{\mathbf{d}}_k$ is:

$$\begin{aligned}p_e\left(\hat{\mathbf{d}}_k/\left|\mathbf{A}_k\right|\right) &= \left(1-\frac{1}{\sqrt{M}}\right)\text{erfc} \\ &\quad\times\left(\sqrt{\frac{3N^2E_s}{2\left(M-1\right)\sigma_w^2\sum_{n=1}^{N}\alpha_{kn}^{-2}}}\right)\end{aligned} \tag{21}$$

There is no ISI appeared in equation (21), because:

- The ML multi-symbols detector estimates the diversity symbols in the observation space (diversity space).
- The noise random variables in the observation vector are independent.
- The ML multi-symbols detector implicitly maps the diversity symbols from the diversity space to the modulated symbols space after estimating the diversity symbols.

The total SNR of the decision variable in the k^{th} diversity period is:

$$\gamma_k = \frac{N^2E_s}{\sigma_w^2\sum_{n=1}^{N}\alpha_{kn}^{-2}} \tag{22}$$

The total SNR in equation (22) is the SNR of the decision variable in the proposed diversity system with UGC receiver. It is smaller than the average SNR of the decision variable at the output of the MRC receiver with the same diversity order, but it is bigger than the average SNR of the decision variable in the systems with no signal diversity. γ_k^{-1} is an inverse chi-square random variable with 2N degrees of freedom. The probability density function of the inverse chi-square random variable is shown in equation (23).

$$p\left(\gamma_k^{-1}\right) = \frac{1}{(N-1)!\left(\bar{\gamma_k^{-1}}\right)^N}\left(\gamma_k^{-1}\right)^{-N-1}e^{-\left(1\Big/\left(\bar{\gamma_k^{-1}}\gamma_k^{-1}\right)\right)} \tag{23}$$

The average inverse signal to noise ratio is:

$$\bar{\gamma_k^{-1}} = \frac{\sigma_n^2}{\text{N}E_s}E\left[\alpha_{kn}^{-2}\right] \tag{24}$$

By averaging the conditional probability of error in equation (21) over the inverse chi-square probability density function of the inverse signal to noise ratio γ_k^{-1}, the average probability of error in the output vectors of the ML multi-symbol detector is shown in equation (25), as shown at the bottom of the next page.

From equation (25), the average probability of error in the estimated vector $\hat{\mathbf{d}}_k$ of the modulated symbols in the proposed diversity system is bigger than the average probability of error in the received symbols in the N channels diversity system with MRC receiver. However, it is smaller than the average probability of error in the systems with no signal diversity.

VII. LINEAR MULTI-SYMBOLS DETECTOR

Linear multi-symbols detector may be used instead of ML multi-symbols detector. The computational complexity of the linear multi-symbols' detector is smaller than the computational complexity of the ML detector. Linear multi-symbols detector such as the decorrelator detector and the MMSE detector perform the function of the diversity decoder. The linear multi-symbols detector maps the observation vectors of the diversity symbols from the diversity space to the modulated symbols space.

When the decorrelator detector is used, the observation vector in equation (12) is multiplied with the inverse of the mapping matrix $\mathbf{S}$. Since $\mathbf{S}$ is a Hadamard orthogonal matrix, its inverse is equal to its transpose. The k^{th} decision vector of the modulated symbols at the output of the decorrelator detector is represented by equation (26).

$$\hat{\mathbf{d}}_k = \mathbf{S}^{\text{T}}\mathbf{y}_k = N.\mathbf{d}_k + \mathbf{S}^{\text{T}}.\mathbf{A}_k^{-1}.\mathbf{w}_k \tag{26}$$

The decorrelator diversity detector combines the corresponding N modulated symbols from the N diversity symbols.

It also combines the noise samples that were scaled with the N independent fading gains. The N independent fading gains are the fading gains on the N time slots through which the N diversity symbols are transmitted. The covariance matrix of the noise vector after the decorrelator detector is shown in equation (27).

$$\boldsymbol{cov}\left(\mathbf{S}^{\mathrm{T}}.\mathbf{A}_{\boldsymbol{k}}^{-1}.\mathbf{w}_{\boldsymbol{k}}\right)=\sigma_w^2\mathbf{S}^{\mathrm{T}}.\left|\mathbf{A}_{\boldsymbol{k}}\right|^{-\mathbf{2}}.\mathbf{S}. \tag{27}$$

The noise enhancement at the output of the diversity decorrelator detector is just due to the combining effect of the noise samples from the N diversity time slots. Therefore, it is concluded that the decorrelator detector enhances both the power of the modulated symbols and the power of the noise due to the combing effect and not the decorrelating effect.

In contrast with what happens with the decorrelator detector in SM-MIMO systems and multiuser systems, the decorrelator detector does not enhance the channel noise in the estimated vector $\hat{\mathbf{d}}_{\boldsymbol{k}}$ in equation (26). Because the noise samples in the observation vector $\mathbf{y}_{\boldsymbol{k}}$ are independent and the diversity-mapping matrix is orthogonal. On the other hand, the noise samples in the observation vector in SM-MIMO systems and multiuser systems are correlated. Moreover, the correlation matrix between the received symbols in SM-MIMO systems and the correlation matrix between the users in multiuser systems are usually non-orthogonal matrices. If the diversity-mapping matrix $\mathbf{S}$ in the proposed system is not orthogonal, the multi-symbol decorrelator will enhance the channel noise in the estimated vector but with an amount less than the decorrelator in SM-MIMO systems and multiuser systems.

The n^{th} element on the decision vector $\left(\mathbf{S}^{\mathrm{T}}\mathbf{y}_{\boldsymbol{k}}\right)$ is:

$$\left(\mathbf{S}^{\mathrm{T}}\mathbf{y}_{\boldsymbol{k}}\right)_n=N.d_{kn}+\sum_{m=1}^{N}s_{nm}.\frac{e^{-j\phi_{km}}.w_{km}}{\alpha_{km}} \tag{28}$$

s_{nm} is the element in the n^{th} row and m^{th} column of the orthogonal matrix $\mathbf{S}$. Since the noise samples w_{km} are uncorrelated, noise variance in the n^{th} decision variable in equation (28) is the summation of the variance of the noise samples in the mapped noise vector $\left(\mathbf{A}_{\boldsymbol{k}}^{-1}.\mathbf{w}_{\boldsymbol{k}}\right)$.

$$\begin{aligned}var\left(\left(\mathbf{S}^{\mathrm{T}}.\mathbf{A}_k^{-1}.\mathbf{w}_{\boldsymbol{k}}\right)_n\right)&=var\left(\sum_{m=1}^{N}\frac{e^{-j\phi_{km}}.w_{km}}{\alpha_{km}}\right)\\&=\sigma_w^2\sum_{m=1}^{N}\alpha_{km}^{-2}\end{aligned} \tag{29}$$

If the noise components in the noise vector $\left(\mathbf{A}_{\boldsymbol{k}}^{-1}.\mathbf{w}_{\boldsymbol{k}}\right)$ are correlated as in the case of SM-MIMO and multiuser systems, the variance of noise in the n^{th} decision variable of the estimated vector of modulated symbols $\left(\mathbf{S}^{\mathrm{T}}\mathbf{y}_{\boldsymbol{k}}\right)$ will be:

$$\begin{aligned}var\left(\left(\mathbf{S}^{\mathrm{T}}.\mathbf{A}_k^{-1}.\mathbf{w}_{\boldsymbol{k}}\right)_n\right)==\sigma_w^2\sum_{m=1}^{N}\alpha_{km}^{-2}\\+\sum_{l\neq m}^{N}\frac{cov\left(w_{km},w_{kl}\right)}{\alpha_{km}.\alpha_{kl}}\end{aligned} \tag{30}$$

From equation (29), no noise enhancement occurs in the used time-diversity system due to the decorrelating process of the decorrelator detector. The variance of the noise after the decorrelator detector is $\sigma_v^2\sum_{m=1}^{N}\alpha_{km}^{-2}$ because the noise samples before the decorrelator detector are uncorrelated. The correlation between the noise samples in the input vector to the decorrelator detector is one of the noise enhancement sources of the decorrelator detector in multiuser systems and SM-MIMO systems.

The behavior of the decorrelator diversity detector is the same as the behavior of the UGC receiver. If we assume that there are N independent fading channels between a transmitter and a receive and the k^{th} modulated symbol is transmitted through these channels, and if we also assume that a separate matched filter is used to detect the received symbol from each channel, the outputs from the N matched filters will be equal to:

$$\begin{aligned}r_{k1}&=\alpha_{k1}e^{j\phi_{k1}}.d_k+w_{k1}\\r_{k2}&=\alpha_{k2}e^{j\phi_{k2}}.d_k+w_{k2}\\&\vdots\\r_{kN}&=\alpha_{kN}e^{j\phi_{kN}}.d_k+w_{kN}\end{aligned} \tag{31}$$

The UGC is used to combine the output symbols from the N-matched filters in one decision variable. The output of the UGC can be represented as shown in equation (32).

$$\begin{aligned}\hat{d}_k^{MRC}&=\sum_{m=1}^{N}\frac{e^{-j\phi_{km}}}{\alpha_{km}}r_{km}\\&=N.d_k+\sum_{m=1}^{N}\frac{e^{-j\phi_{km}}.w_{km}}{\alpha_{km}}\end{aligned} \tag{32}$$

The UGC combines the modulated symbols with unity gains in one decision variable. It is simpler than the MRC, but its performance is not optimum. The average noise power in the decision variable of the UGC is smaller than the average noise power in the decision variable of the system with no signal diversity, but it is bigger than the average noise power in the

$$\begin{aligned}\bar{p_e}\left(\hat{\mathbf{d}}_{\mathrm{k}}\right)&=\frac{\left(\sqrt{M}-1\right)}{\sqrt{M}\,(N-1)!\left(\bar{\gamma_k}^{-1}\right)^N}\int_0^{\infty}\mathrm{erfc}\left(\sqrt{\frac{3}{2\,(M-1)\,\gamma_k^{-1}}}\right).\left(\gamma_k^{-1}\right)^{-N-1}e^{-\left(1/\left(\bar{\gamma_k}^{-1}\gamma_k^{-1}\right)\right)}.d\gamma_k^{-1}\\&=\left(1-\frac{1}{\sqrt{M}}\right)\left[\frac{1}{2}\left(1-\sqrt{\frac{3}{2\,(M-1)\,\bar{\gamma_k}^{-1}+3}}\right)\right]^{N+1}\sum_{n=0}^{N-1}\binom{N-1+n}{n}\left[\frac{1}{2}\left(1+\sqrt{\frac{3}{2\,(M-1)\,\bar{\gamma_k}^{-1}{}_k+3}}\right)\right]^n\end{aligned} \tag{25}$$

decision variable of the MRC receiver. The performance of the UGC will be the same as the performance of the MRC if the fading gains in the N diversity channels are the same or closed to each other.

Although the MRC receiver is the optimum combining method used in the diversity systems, it cannot be used in time-diversity system without reducing the bandwidth efficiency of the transmitted symbols. On the other hand, the diversity gain in the proposed UGC is less than the diversity gain of the MRC, but it can be used with the proposed time-diversity system, which does not reduce the transmission rate of the modulated symbols or the bandwidth efficiency of the transmitted symbols due the used time-diversity method. Consequently, the proposed time-diversity system with UGC receiver achieves diversity gain and its bandwidth efficiency is the same as the bandwidth efficiency of the systems with no signal diversity.

By comparing equation (32) and equation (28), we conclude that the output of the decorrelator diversity decoder in the receiver of the proposed time-diversity system is the same as the output of the UGC receiver with N independent fading channels. If the output of the decorrelator diversity detector is divided by N, the decision variable for the n^{th} modulated symbol in the k^{th} modulated vector will be:

$$\begin{aligned}\hat{d}_{kn} &= \frac{1}{N}.\left(\mathbf{S}^{\mathrm{T}}\mathbf{y}`_{k}\right)_{n} \\ &= d_{kn} + \frac{1}{N}.\sum_{m=1}^{N} s_{nm}.\frac{e^{-j\phi_{km}}.w_{km}}{\alpha_{km}} \end{aligned} \tag{33}$$

Increasing the time-diversity order in the proposed system does not enhance the noise after the decorrelator detector. From equation (33), the averaging of noise samples in the output of the decorrelator detector lowers the noise variance. Therefore, increasing the time-diversity order increases the averaging interval of noise samples and further decreases the noise power. This is the source of performance improvement in the proposed diversity system. However, in SM-MIMO, the increase of the spatial multiplexing order enhances the noise after the decorrelator detector. In a multiuser system, the increase in the number of users also enhances the noise power at the output of the decorrelator detector.

In the proposed receiver, the baseband demodulator uses the decision variable in equation (33) to estimate the data symbol corresponding to the n^{th} estimated modulated symbol in the k^{th} vector $\hat{\mathbf{d}}_{\boldsymbol{k}}$. The upper bound of the conditional probability of error in estimating the n^{th} modulated symbol is:

$$\begin{aligned} p_e &\left(\hat{\mathrm{d}}_{kn}/\alpha_{k1}^{-2}, \alpha_{k2}^{-2}, \ldots, \alpha_{kN}^{-2}\right) \\ &= \left(1 - \frac{1}{\sqrt{M}}\right)\mathrm{erfc} \\ &\quad \times \left(\sqrt{\frac{3N^2.E_s}{2\left(M-1\right)\sigma_w^2\sum_{m=1}^{N}\alpha_{km}^{-2}}}\right) \end{aligned} \tag{34}$$

E_s is the average energy of the constellation points in the used modulation scheme. M is the modulation order. By comparing equations (34) and (21), it is found that the instantaneous conditional probability of error in the estimated symbols when the decorrelator detector is used, is the same as the instantaneous conditional probability of error in the estimated symbols when the ML detector is used. Two reasons explain this performance. The first is the usage of the orthogonal diversity matrix to map the modulated symbols vectors to the diversity symbols vectors. The second reason is that the diversity symbols are transmitted in orthogonal N time slots.

The instantaneous SNR of the n^{th} estimated symbol of the k^{th} output vector from the decorrelator diversity detector is:

$$\gamma_{kn} = \frac{N^2.E_s}{\sigma_w^2\sum_{m=1}^{N}\alpha_{km}^{-2}} \tag{35}$$

The inverse SNR is equal to that shown in equation (22). It is an inverse chi-square random variable with 2N degrees of freedom. The average inverse SNR is equal to that shown in equation (24) too. By using the probability density function of the inverse chi-square random variable in equation (23), the average probability of error in estimating the k^{th} vector of modulated symbols is shown in equation (36), as shown at the bottom of the next page.

From equation (36), the average probability of error in the estimated symbol $\hat{\mathrm{d}}_{kn}$ in the used time-diversity system is the same as the average probability of error in N channels diversity system with UGC receiver. By comparing the average probability of error in equations (36) and (25), the performance of the multi-symbol decorrelator detector in the proposed time-diversity system when orthogonal mapping matrix is used, is the same as the performance of the ML detector. The reasons behind this are:

1- The independence between the noise components in the decision vector at the output of the fading compensator.
2- The choice of the diversity-mapping matrix to be symmetric and orthogonal.

Figure (4) shows a comparison between the bit-error-rate (BER) performance of the ML detector and the decorrelator detector with the proposed time-diversity system in Rayleigh flat fading channel. The average probability of error in the proposed time-diversity system that uses orthogonal diversity encoder and diversity symbols interleaving, is the same as the average probability of error in a UGC receiver with N diversity channels. However, the average probability of error of the proposed time-diversity system is bigger than the average probability of error of an MRC receiver with N diversity channels. The proposed time-diversity system with a UGC receiver can achieve a maximum diversity gain equal to $10\log_{10}(N)$ dB with respect to the systems with no signal diversity. This diversity gain is achieved without reducing the bandwidth efficiency of the transmitted symbols. Moreover, the performance of the ML detector in the proposed time-diversity system is the same as the performance of the decorrelator detector. Figure (4) has a surprising observation. The BER performance of the proposed system is significantly enhanced with the AWGN channel. The reason for this

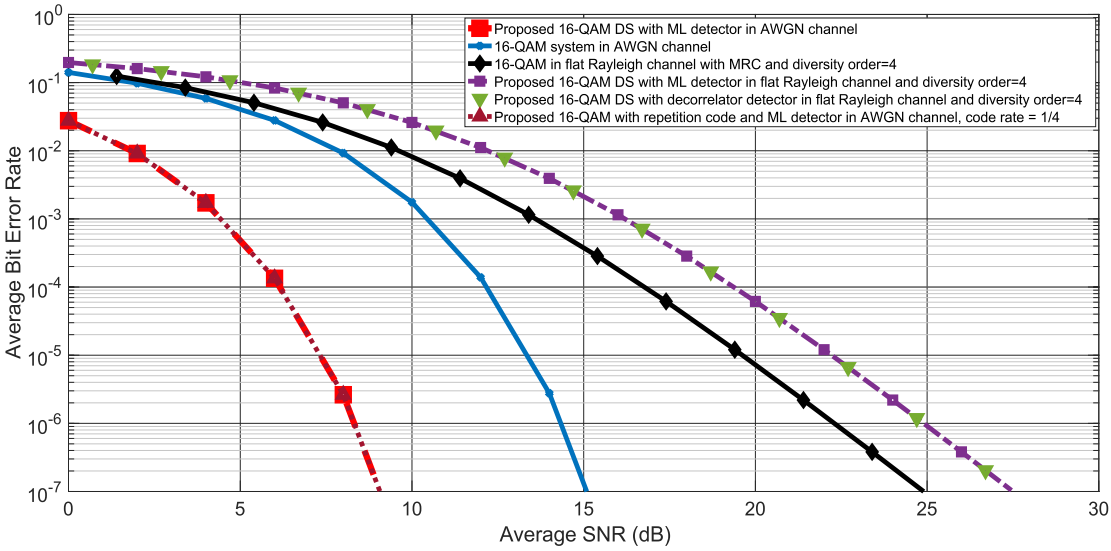

FIGURE 4. Comparison between conventional 16-QAM and proposed 16-QAM-diversity systems in AWGN and flat Rayleigh channel, the used diversity order is 4.

enhancement is that the transmission of each modulated symbol through N time slots is similar to the usage of a repetition code in the AWGN channel. The order of the repetition code is equal to the time-diversity order. When a repetition code is used in the conventional systems, the symbols transmission rate is reduced, but in the proposed system, the transmission rate of modulated symbols is reserved. Therefore, it is concluded from figure (4) that the energy E_s of the decision variable in the used time-diversity system increases by $10\log_{10}(N)$ dB, where N is the time-diversity order.

VIII. RESULTS AND DISCUSSIONS

In this section, the proposed time-diversity system is simulated with Rayleigh flat fading channel at different time-diversity orders. The target data rates in the simulated systems are 50 M bits/s and 100 M bits/s. The used modulation schemes are QPSK and 16-QAM. The transmission bandwidth is 25 MHz. The coherence bandwidth of the used fading channel is 27 MHz. The coherence time of the channel is equal to 1 ms, which is corresponding to a maximum doppler-shift of 1 kHz. In the receiver, the symbol-timing recovery is done using the Mü ller and Mueller algorithm. The estimation of the coarse carrier frequency offset is done using the Fast-Fourier Transform (FFT) algorithm; however, the estimation of the fine carrier frequency offset is done using pilot symbols in the header of each frame of symbols. The symbols frame consists of 512 diversity symbols. 16 pilot symbols are attached in the beginning of each frame. According to equation (5), the symbol interleaving width is 25000 diversity vectors, and its depth is equal to the used time-diversity order. The system is simulated for 4, 8, and 16 time-diversity orders. The big benefit of the used time-diversity scheme is the high time-diversity order that can be achieved without affecting the transmission rate and the transmission bandwidth. The proposed diversity system uses the same transmission rate and bandwidth as the systems with no signal diversity, whatever the used order of time diversity.

MATLAB m-files are written to simulate the proposed time-diversity system. Two approaches are used to evaluate the performance of the proposed system. The first approach is the received average BER versus the received average SNR. The second approach is a comparison between the noise power in the decision vector and the noise power in the observation vector. The simulations are done using two different receivers. The first receiver uses the ML detector and the second receiver uses the linear decorrelator detector. The performance of the simulated systems is compared with the performance of the optimum N diversity channels system with MRC receiver and ML detector.

$$\bar{p_e}\left(\hat{\mathrm{d}}_{kn}\right) = \frac{\left(\sqrt{M}-1\right)}{\sqrt{M}\,(N-1)!\bar{\gamma}_k^N}\int_0^\infty \mathrm{erfc}\left(\sqrt{\frac{3\gamma_k}{2\,(M-1)}}\right).\gamma_k^{N-1}e^{-\frac{\gamma_k}{\bar{\gamma}_k}}.d\gamma_k$$
$$= \frac{\left(\sqrt{M}-1\right)}{\sqrt{M}}\left[\frac{1}{2}\left(1-\sqrt{\frac{3\bar{\gamma}_k}{2\,(M-1)+3\bar{\gamma}_k}}\right)\right]^N\sum_{n=0}^{N-1}\binom{N-1+n}{n}\left[\frac{1}{2}\left(1+\sqrt{\frac{3\bar{\gamma}_k}{2\,(M-1)+3\bar{\gamma}_k}}\right)\right]^n \quad (36)$$

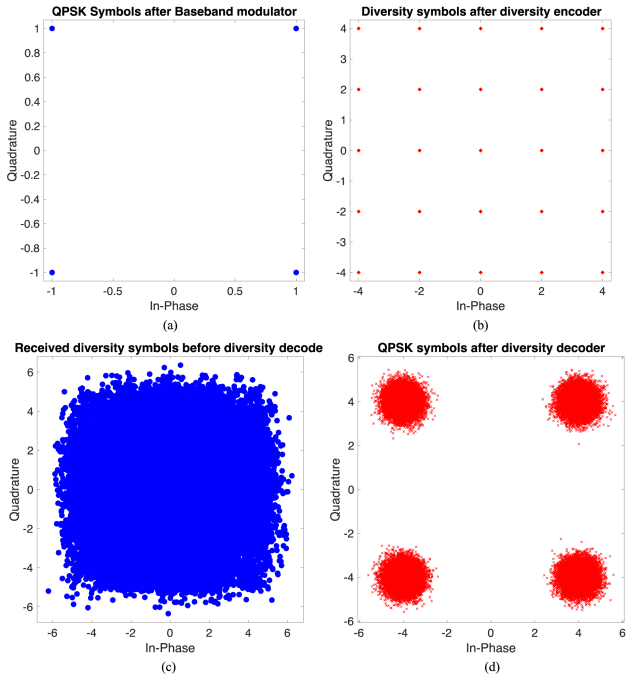

FIGURE 5. The constellation diagram of the modulated symbols and the diversity symbols before and after the diversity encoder and the diversity decoder in a QPSK system, the used diversity order is 4. (a) Constellation symbols at modulator output. (b) Constellation symbols at diversity encoder output. (c) Constellation symbols at diversity decoder input. (d) Constellation symbols at demodulator input.

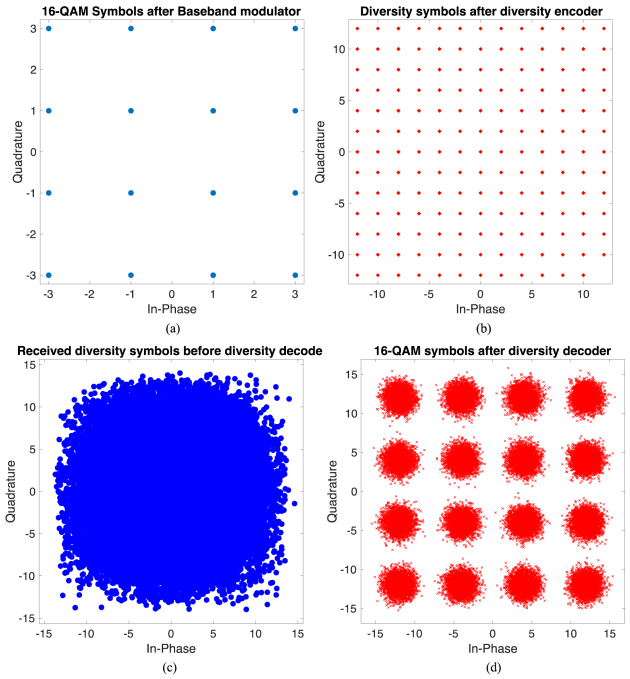

FIGURE 6. The constellation diagram of the modulated symbols and the diversity symbols before and after the diversity encoder and the diversity decoder in a 16-QAM system, the used diversity order is 4. (a) Constellation symbols at modulator output. (b) Constellation symbols at diversity encoder output. (c) Constellation symbols at diversity decoder input. (d) Constellation symbols at demodulator input.

Figures (5) and (6) show the constellations diagrams of the modulated symbols and the diversity symbols before and after the diversity encoder and the diversity decoder. QPSK modulation is used in figure (5), and 16-QAM modulation is used in figure (6). In figure (5.a) and (6.a), the constellations points before the diversity encoder are represented for QPSK system and 16-QAM system, respectively. The diversity symbols after the diversity encoders in both systems are represented in figures (5.b) and (6.b). The two systems use Hadamard orthogonal matrix of order 4. As expected, the size of the constellation diagram of the diversity symbols is bigger than the size of the constellation diagram of the modulated symbols. The constellations sizes are increased by increasing the diversity order. Figures (5.c) and (6.c) represent the received diversity symbols before the diversity decoders in both systems. The constellations points in these figures are affected by the channel noise and the channel fading. The average SNR in both systems is 20 dB. Finally, figures (5.d) and (6.d) represent the received modulated symbols after the diversity decoders in both systems. The diversity decoders removed the interferences occurred by the diversity encoder in the transmitter. They also return the constellation size of the modulated symbols to the normal size of each modulation scheme. The modulated symbols in figures (5.d) and (6.d) are merely affected by the channel noise.

Figure (7) shows the average BER in the received data symbols that come out from the proposed time-diversity system at different diversity orders. The used modulation scheme in this simulation is QPSK. Figure (7) also shows the average BER in the received data symbols from the optimum time-diversity system with N diversity channels and MRC receiver. From the simulation results in figure (7), it is observed that the average BER performance of the proposed time-diversity system is worse than the average BER performance of the optimum N channels diversity system with MRC receiver by 2.5 dB for diversity order 4, 2 dB for diversity order 8, and 1.5 dB for diversity order 16. This performance lose is due to the usage of UGC in the receiver of the proposed system, which is affected significantly by the gains of the fading channels more than the MRC receiver. Moreover, the BER performance of the linear decorrelator detector in the proposed system is the same as the BER performance of the ML detector because of the reasons mentioned in section 7. Therefore, the decorrelator detector can be used in place of the ML detector in the proposed time- diversity receiver to take advantage of its low complexity. The simulation results in figure (7) match the mathematical results, which are represented in sections (5), (6), and (7). Figure (8) shows the same performance curves of the proposed time-diversity system and the MRC receiver but when 16-QAM modulation is used. The same results and conclusions are obtained from figure (8) as those in figure (7). The relative performance of the proposed time-diversity system is not affected by changing in modulation order.

The time-diversity method in the proposed system works like the repetition channel coding in the systems with no signal diversity. The proposed system is compared with a QAM system with repetition code in AWGN channel

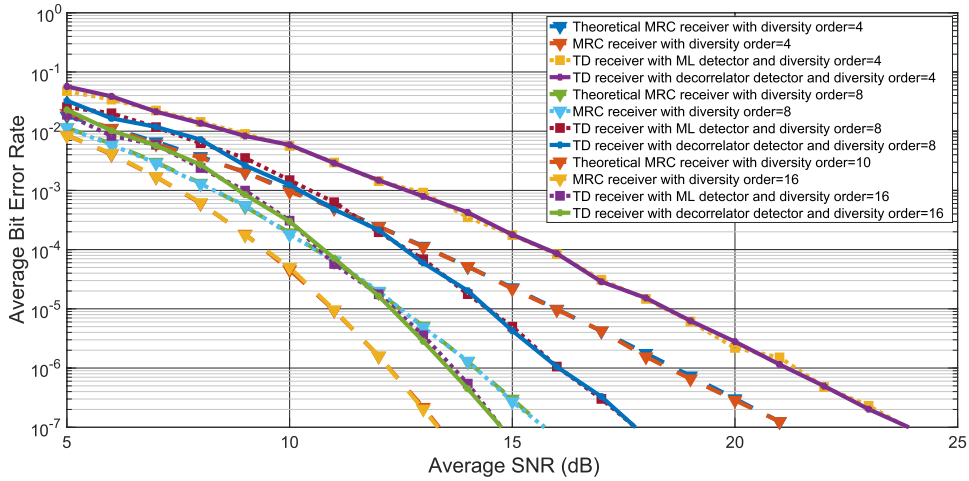

FIGURE 7. BER comparison between the proposed time-diversity system and the *N* channels diversity systems with MRC receiver using QPSK.

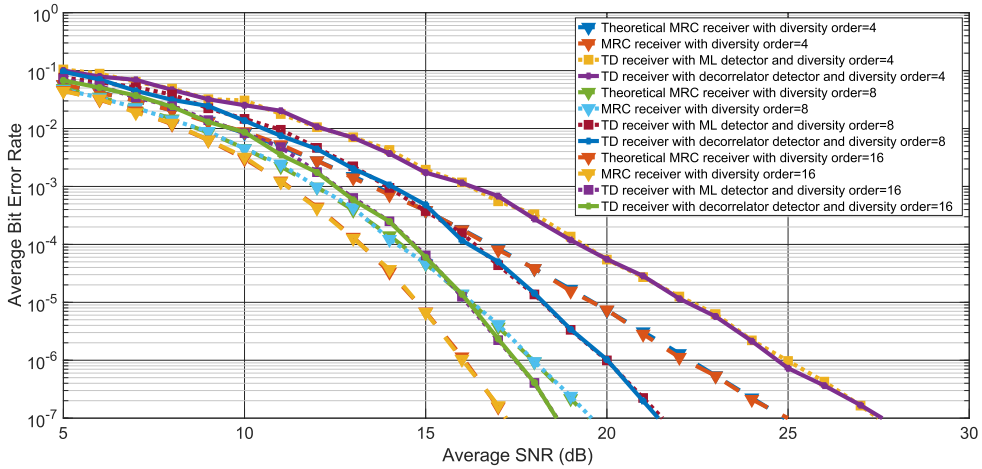

FIGURE 8. BER comparison between the proposed time-diversity system and the *N* channels diversity systems with MRC receiver using 16-QAM.

and in Rayleigh flat-fading channel. Figure (9) shows the comparison between the BER performance of the proposed system with 16-QAM modulation and diversity order 4 and the BER performance of the conventional 16-QAM system with repetition code. The code rate of the repetition code is 1/4. There is no signal diversity used in the conventional coded 16-QAM system. It is well known that when the repetition code is used in channel coding, it is preferred to have an odd number of symbol repetitions. However, an even number of repeated symbols is used in the simulation to be the same as the diversity order of the proposed system, which must be an even number due to the characteristics of the Hadamard orthogonal matrix. From figure (9), the BER performance of the proposed time-diversity system is 3 dB better than the performance of the coded 16-QAM system in AWGN channel. This is because the UGC in the proposed receiver increases the SNR of the decision variable by 6 dB and the code gain in the receiver of the coded 16-QAM system is 3 dB. The receiver of the coded 16-QAM system decides a symbol error if two or three or four symbols' errors occur in the received coded symbols.

In Rayleigh flat-fading channel, the BER performance of the coded 16-QAM system is better than the BER performance of the proposed system at low SNR. But at high SNR, the BER performance of the proposed system outperforms the BER performance of the coded 16-QAM. This is because at high SNR, the UGC in the proposed receivers increases the average SNR of the decision variable more than the code gain of the coded 16-QAM system. The BER performances of the proposed system and the coded 16-QAM system are also compared with the BER performance of the optimum time-diversity system with MRC receiver. The BER performance of the coded 16-QAM cannot outdo the BER performance of the optimum time-diversity system.

Although the performance of the coded 16-QAM system is better than the performance of uncoded 16-QAM system by 3 dB, the rate of symbols transmission and the bandwidth

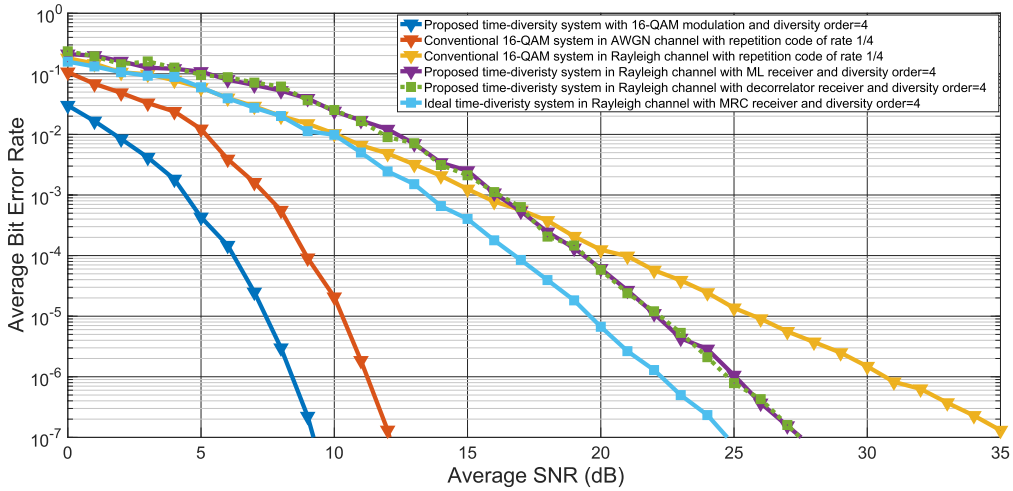

FIGURE 9. BER comparison between the proposed time-diversity system and the coded 16-QAM system with repetition code rate 1/4 in AWGN channel and Rayleigh flat-fading channel.

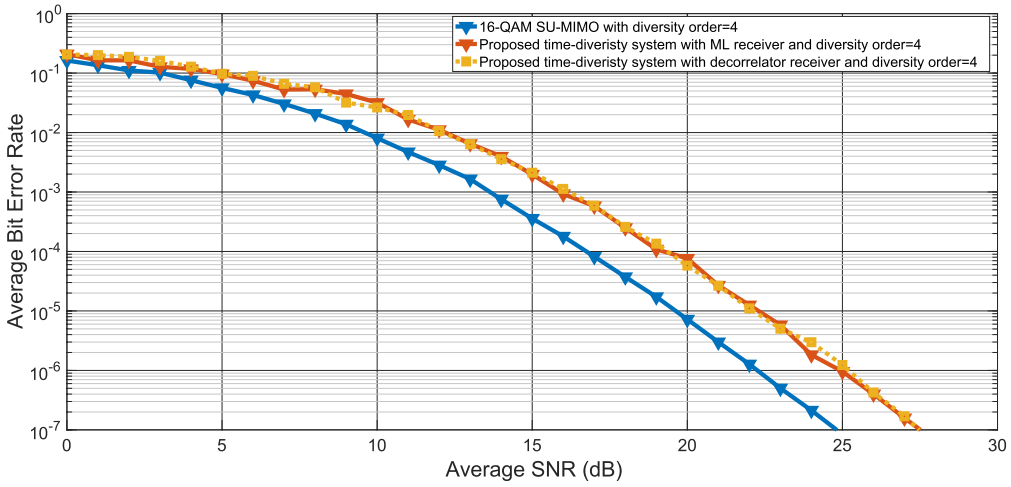

FIGURE 10. BER comparison between the proposed time-diversity system and the SU-MIMO system in Rayleigh flat-fading channel.

efficiency of the coded 16-QAM system is 1/4 of the symbols transmission rate and the bandwidth efficiency of the uncoded 16-QAM system. In the proposed system, the achieved diversity gain, and the improvement in the BER performance come without reducing the rate of symbols transmission or reducing the bandwidth efficiency of the system.

Figure (10) shows the comparison between the proposed time-diversity system and a single-user MIMO (SU-MIMO) system. Both systems use 16-QAM modulation. The SU-MIMO system uses a space-diversity with diversity order 4. The SU-MIMO system uses an MRC receiver to combine the 4 space-diversity symbols from the 4 channel paths into one decision variable. The diversity order of the proposed time-diversity system is 4, and it uses a UGC receiver to combine the time diversity symbols into one decision variable. The BER performance curves in figure (10) show that the performance of the SU-MIMO system with MRC receiver is the same as the performance of the optimum N channels diversity system with MRC. However, the performance of the proposed time-diversity system is worse than the performance of the SU-MIMO system by 2.5 dB. This performance degradation is due to the using of the UGC receiver in the proposed system instead of the MRC receiver in the SU-MIMO. As it is shown in sections 6 and 7, the UGC is a sub-optimum combining method, however the MRC is the optimum combining method. The BER performance improvement in the SU-MIMO from the space-diversity gain comes by increasing the number of the transmitting antennas and the number of the receiving antennas. In the simulated SU-MIMO system, two transmitting antennas are used with two power amplifiers and two driving circuits. Two receiving antennas with two matching circuits and two low-noise amplifiers are also used in the receiver. On the other hand, the diversity gain in the proposed system comes by using one transmitting antenna and one receiving antenna. In the SU-MIMO system the number of the used antennas

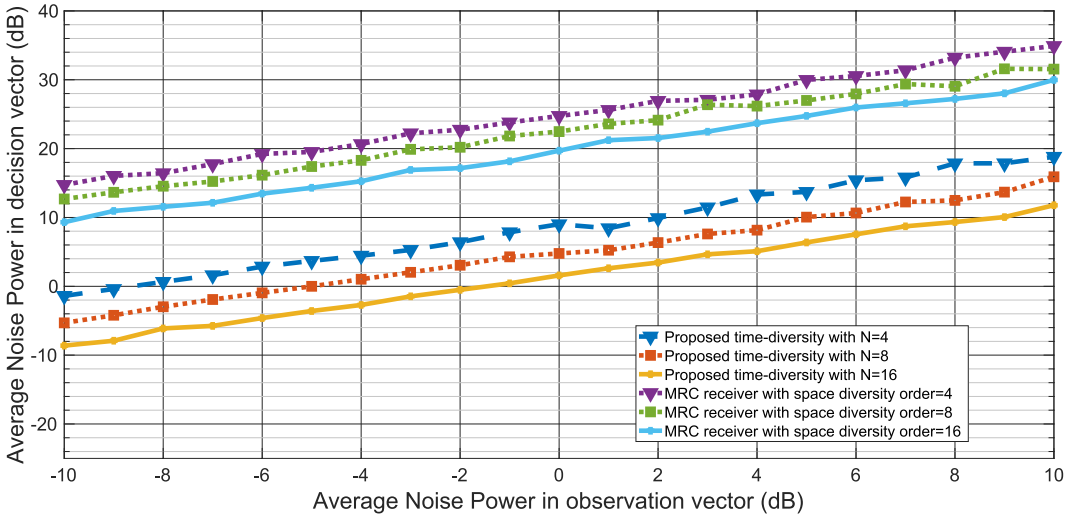

FIGURE 11. Comparison between the noise variance in the decision variable of the decorrelator multi-symbol detector in the proposed time-diversity receiver and SU-MIMO with MRC receiver.

increases linearly with the space-diversity order, but in the proposed time-diversity system, one transmitting antenna and one receiving antenna are used whatever the value of the time-diversity order is. In the proposed system, the rate of the transmitted symbols does not affect with the time-diversity order, and it is equal to one symbol per channel use. However, in the SU-MIMO system the transmission rate is one symbol by channel use as long as the number of transmitting antennas is less than or equal to 4, and it decreases when the number of the transmitting antennas increases more than 4.

The improvement in the BER performance of the decorrelator detector in the proposed time-diversity system is due to that the noise samples in the observation vector are independent, and the diversity mapping matrix is orthogonal. If the decorrelator detector is used in the SU-MIMO system with the MRC receiver, it will enhance the noise power in the decision vector. This noise enhancement is due to two factors. The first is the correlation between the noise samples in the observation vector of the MRC receiver. The second factor is the correlation matrix between the received symbols from the N channels of the SU-MIMO system, which is not orthogonal. Figure (11) shows the variation of the noise power in the decision vector with the noise power in the observation vector when the decorrelator detector is used in the proposed system and SU-MIMO system.

The last method of performance evaluation measures the average BER in real-time implemented systems. Xilinx FPGA embedded platform is used to implement both the proposed time-diversity system and an N channels diversity system with an MRC receiver. The transmitters and the receivers of the two systems are implemented on 4 FPGA kits in the lab. The fading channel gains are taken from a time-varying channel emulator, which is implemented on a separated FPGA kit and configured by a computer software. The channel parameters, which should be specified to the software of the channel emulator, are the coherence bandwidth, the multipath-delay profile, the Doppler frequency shift, the probability density function (pdf) of the channel gains, the mean of the channel gains, the variance of the channel gains, and the correlation matrix between the fading gain if MIMO transmission is used. The rate of the transmitted samples from the transmitter must be specified to the fading emulator. The FPGA kit of the channel emulator takes the transmitted samples from the FPGA kit of the transmitter and applies the channel model on these samples according to the specified channel parameters, then it sends the faded samples to the FPGA kit of the receiver. Before sending the samples of the channel output to the receiver, the sampling rate is changed in the last stage inside the channel emulator kit. The rate by which the receiver reads its input samples must be specified to the channel emulator to perform the required sampling rate conversion. In the simulated systems, the output sampling rate of the transmitter is 8X (X is equal to the symbol rate R_s). The sampling rate in the channel emulator is 8X too. The sampling rate of the receiver input is 4X. Therefore, the channel emulator will decimate the rate of its output samples by 2.

Two receivers for the proposed time-diversity system are implemented using the ML detector and the linear decorrelator detector. The average BER values in the received data symbols from the implemented receivers are calculated at six received average SNRs (0 dB, 5 dB, 10 dB, 15 dB, 20 dB, and 25 dB). Figure (12) shows that the BER performance curves of the two diversity systems are identical. This result matches those of the simulated systems in figure (7) and the result of the mathematical verification done for the proposed system. Figure (12) also shows that the BER performance of the proposed time-diversity system is suboptimum compared to the BER performance

TABLE 2. Synthesis results of the implemented time-diversity system and the conventional 16-QAM system.

Resource	Available	The conventional 16-QAM system with time-diversity order 16 and MRC receiver			The Proposed 16-QAM system with time-diversity order 16		
		Transmitter	Receiver	Utilization %	Transmitter	Receiver	Utilization %
LUT	303600	31847	33541	21.53	35826	47328	27.38
FF	607200	58372	76434	22.2	116238	147363	43.41
IO	700	24	24	6.8	24	24	6.8
BUFG	32	4	7	36.67	7	9	50
Worst negative slack		1.121 ns	0.087 ns		0.93 ns	0.0391 ns	
Worst hold slack		0.064ns	0.046 ns		0.041 ns	0.013 ns	

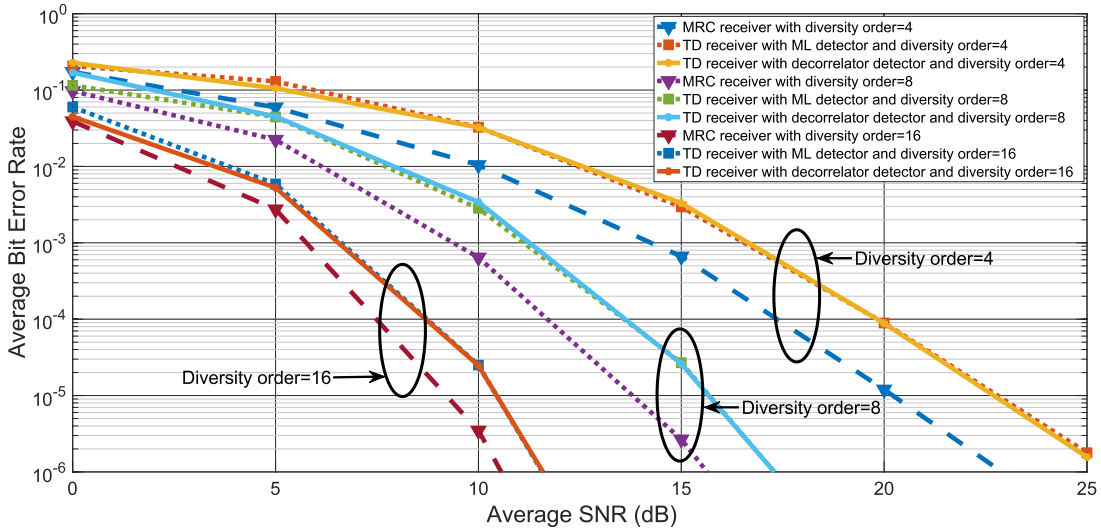

FIGURE 12. BER performance of the real-implemented time-diversity system and real-implemented *N* channels diversity system using Xilinx FPGA embedded system.

TABLE 3. The fixed-point representation of the interface samples.

Samples	Fixed-Point representation
Transmitter output	1 sign bit, 5 integer bits, 6 fraction bits
Channel emulator	1 sign bit, 5 integer bits, 6 fraction bits
Receiver output	1 sign bit, 7 integer bits, 8 fraction bits

TABLE 4. The fixed-point representation extremes.

Samples	Transmitter	Receiver
Minimum representation	1 sign bit, 3 integer bits, 3 fraction bits	1 sign bit, 5 integer bits, 7 fraction bits
Maximum representation	1 sign bit, 11 integer bits, 12 fraction bits	1 sign bit, 11 integer bits, 12 fraction bits

of the optimum *N* channels diversity system with MRC receiver.

Table 2. lists the synthesis results of the used time-diversity system and the conventional 16-QAM system with the MRC receiver. The used Xilinx platform is Vitex-7 VC707. The complexity of the proposed system is bigger than the complexity of the conventional diversity system that uses the same modulation scheme and diversity order. This is the cost that should be paid in the proposed system to enhance the BER performance using time-diversity without affecting the transmission rate or the bandwidth efficiency. In the following, some hints are given about the hardware of the implemented systems. However, the details of the used architectures in implementing the proposed and conventional systems in Table 2 are represented in another work. The implemented architectures use the signed fixed-point representation to represent the samples of the signals inside the transmitter, the channel emulator, and the receiver. Table 3 shows the fixed-point representation of the samples at the transmitter output, the channel emulator, and the receiver input.

Table 4 shows the extremes of the fixed-point representations of the samples inside the transmitter and the receiver.

The maximum sample representation is almost used to represent the samples at the output of the convolution process or the inner product of vectors. However, the minimum sample representation is almost used to implement some constants such as the filters coefficients.

IX. CONCLUSION

The proposed time-diversity system with a UGC receiver achieves a suboptimal BER performance compared to the BER performance of an optimal N channel diversity system with an MRC receiver. The proposed system uses one transmitting antenna and one receiving antenna. The proposed time-diversity system achieves full diversity without affecting the transmission rate of the modulated symbols. Moreover, the bandwidth of the transmitted symbols from the proposed time-diversity system is the same as the bandwidth of the transmitted symbols from the non-diversity system that uses the same modulation scheme and symbols rate. The proposed system transmits one symbol per channel used for any used time-diversity order. The transmitter of the proposed system uses a diversity encoder to generate N diversity symbols from N modulated symbols. The diversity symbols are stored in an interleaving memory of depth N and width equal to the coherence time of the channel. The interleaved diversity symbols from the same diversity vectors are transmitted in different time slots that have independent fading gains. The symbol deinterleaving and the diversity decoder are used in the receiver to combine the corresponding modulated symbols from the received diversity symbols.

The proposed time-diversity system is suitable for working in flat-fading channels with fast and slow fading. The interleaving stage is used to adjust the diversity period according to the channel coherence time. In slow fading environments, the width of the interleaving memory is big to allow the diversity symbols from the same diversity vector to have independent fading gains. However, in fast fading environments, the width of the interleaving memory is low because the coherence time of the channel is low. The controller of the physical layer is responsible for setting the width of the interleaving and deinterleaving memories.

Due to the nature of the proposed time-diversity system, the noise samples in the observation vector to the multi-symbol detector are independent. We exploited this observation and proved by mathematics, simulations, and real implementations that the BER performance of the ML multi-symbol detector is the same as the BER performance of the decorrelator multi-symbol detector in the proposed time-diversity receiver. Therefore, we can use the decorrelator multi-symbol detector, which has lower computational complexity, instead of the ML detector, which has higher computational complexity. The complexity of the proposed time-diversity system is less than the complexity of any corresponding system, which achieves the same diversity gain and transmission rate. However, due to the used symbol interleaving/deinterleaving and the diversity encoder/decoder, the complexity of the proposed time-diversity system is higher than the complexity of the non-diversity system that uses the same modulation scheme and transmission rate.

In future work, the implementation architectures of the proposed time-diversity system with UGC receiver and the conventional time-diversity system with MRC receiver are represented in detail. All implementation issues of the two systems will also be represented in this work with a full detailed analysis of system complexity and its power consumption. The effects of imperfect CSI estimation will also be studies in a separate work. The recommended estimation algorithms for the CSI will be proposed. The BER performance of the proposed system in the existence of the channel estimation error will be represented in this work.

REFERENCES

[1] M. Surendar and P. Muthuchidambaranathan, "Low complexity and high diversity gain non-linear constellation precoded MIMO-OFDM system with subcarrier grouping," *AEU Int. J. Electron. Commun.*, vol. 70, no. 3, pp. 265–271, Mar. 2016.

[2] S. Ki Yoo, S. L. Cotton, W. G. Scanlon, and G. A. Conway, "An experimental evaluation of switched combining based macro-diversity for wearable communications operating in an outdoor environment," *IEEE Trans. Wireless Commun.*, vol. 16, no. 8, pp. 5338–5352, Aug. 2017, doi: 10.1109/TWC.2017.2709298.

[3] K. Zhai, Z. Ma, and X. Lei, "Closed-formed distribution for the SINR of MMSE-detected MIMO systems and performance analysis," *AEU-Int. J. Electron. Commun.*, vol. 97, pp. 16–24, Dec. 2018.

[4] H. Suganuma, S. Saito, T. Maruko, and F. Maehara, "Inter-symbol interference suppression scheme employing periodic signals in coded network MIMO-OFDM systems," in *Proc. IEEE Radio Wireless Symp. (RWS)*, Jan. 2017, pp. 42–44, doi: 10.1109/RWS.2017.7885940.

[5] U. Afsheen, P. A. Martin, and P. J. Smith, "Space time state trellis codes for MIMO systems using reconfigurable antennas," *IEEE Trans. Commun.*, vol. 63, no. 10, pp. 3660–3670, Oct. 2015, doi: 10.1109/TCOMM.2015.2462347.

[6] G. Lei, Y. Liu, and X. Xiao, "Performance analysis of adaptive space-time coded systems with continuous phase modulation," *AEU Int. J. Electron. Commun.*, vol. 80, pp. 80–85, Oct. 2017.

[7] J. Koo, S.-Y. Kim, and J. Kim, "A parallel collaborative sphere decoder for a MIMO communication system," *J. Commun. Netw.*, vol. 16, no. 6, pp. 620–626, Dec. 2014, doi: 10.1109/JCN.2014.000108.

[8] G. M. F. Silva, J. C. M. Filho, and T. Abrão, "Sequential likelihood ascent search detector for massive MIMO systems," *AEU Int. J. Electron. Commun.*, vol. 96, pp. 30–39, Nov. 2018.

[9] D. Gozalvez, D. Gomez-Barquero, D. Vargas, and N. Cardona, "Combined time, frequency and space diversity in DVB-NGH," *IEEE Trans. Broadcast.*, vol. 59, no. 4, pp. 674–684, Dec. 2013, doi: 10.1109/TBC.2013.2281665.

[10] P. Bindu and M. G. Jibukumar, "Diversity embedded rate configurable GSM and a low complexity detection method," *AEU Int. J. Electron. Commun.*, vol. 88, pp. 166–173, May 2018.

[11] J. Lin, T. Pande, I. H. Kim, A. Batra, and B. L. Evans, "Time-frequency modulation diversity to combat periodic impulsive noise in narrowband powerline communications," *IEEE Trans. Commun.*, vol. 63, no. 5, pp. 1837–1849, May 2015, doi: 10.1109/TCOMM.2015.2411601.

[12] S.-B. Lee, I. Pefkianakis, S. Choudhury, S. Xu, and S. Lu, "Exploiting spatial, frequency, and multiuser diversity in 3GPP LTE cellular networks," *IEEE Trans. Mobile Comput.*, vol. 11, no. 11, pp. 1652–1665, Nov. 2012, doi: 10.1109/TMC.2011.206.

[13] A. Y. Hassan, "Code-time diversity for direct sequence spread spectrum systems," *Wireless Pers. Commun.*, vol. 84, no. 1, pp. 695–718, Sep. 2015, doi: 10.1007/s11277-015-2656-z.

[14] A. Y. Hassan, "A simple transmit diversity system for fading channels using shaped sinusoidal functions," *AEU Int. J. Electron. Commun.*, vol. 76, Jun. 2017, pp. 97–106, doi: 10.1016/j.aeue.2017.03.024.

[15] Z. Zhang, J. Chen, and J. Hu, "Energy-efficient massive MIMO system analysis: From a circuit power perspective," in *Proc. IEEE Int. Conf. Digit. Signal Process. (DSP)*, Oct. 2016, pp. 350–354, doi: 10.1109/ICDSP.2016.7868577.

[16] E. Bjornson, L. Sanguinetti, J. Hoydis, and M. Debbah, "Optimal design of energy-efficient multi-user MIMO systems: Is massive MIMO the answer?" *IEEE Trans. Wireless Commun.*, vol. 14, no. 6, pp. 3059–3075, Jun. 2015, doi: 10.1109/TWC.2015.2400437.

[17] S.-Y. Jung and B. W. Kim, "Near-optimal low-complexity antenna selection scheme for energy-efficient correlated distributed MIMO systems," *AEU Int. J. Electron. Commun.*, vol. 69, no. 7, pp. 1039–1046, Jul. 2015.

[18] A. Alfakhri, M. A. Ashraf, A. Alasaad, and S. Alshebeili, "A compact size ultra-wideband MIMO antenna with simple decoupling structure," in *Proc. 17th Int. Symp. Antenna Technol. Appl. Electromagn. (ANTEM)*, Jul. 2016, pp. 1–2, doi: 10.1109/ANTEM.2016.7550170.

[19] C. K. Ghosh, "A compact 4-channel microstrip MIMO antenna with reduced mutual coupling," *AEU Int. J. Electron. Commun.*, vol. 70, no. 7, pp. 873–879, Jul. 2016.

[20] J. Ryckaert, C. Desset, A. Fort, M. Badaroglu, V. De Heyn, P. Wambacq, G. Van der Plas, S. Donnay, B. Van Poucke, and B. Gyselinckx, "Ultra-wide-band transmitter for low-power wireless body area networks: Design and evaluation," *IEEE Trans. Circuits Syst. I, Reg. Papers*, vol. 52, no. 12, pp. 2515–2525, Dec. 2005, doi: 10.1109/TCSI.2005.858187.

[21] H. Werfelli, M. Chaoui, M. Lahiani, and H. Ghariani, "Receiver design for UWB communications," in *Proc. 1st Int. Conf. Adv. Technol. Signal Image Process. (ATSIP)*, 2014, pp. 544–549, doi: 10.1109/ATSIP.2014.6834674.

[22] L. A. Dalton and C. N. Georghiades, "A full-rate, full-diversity four-antenna quasi-orthogonal space-time block code," *IEEE Trans. Wireless Commun.*, vol. 4, no. 2, pp. 363–366, Mar. 2005, doi: 10.1109/TWC.2004.842945.

[23] L.-Y. Song and A. G. Burr, "General differential modulation scheme for quasi-orthogonal space-time block codes with partial or full transmit diversity," *IET Commun.*, vol. 1, no. 2, pp. 256–266, Apr. 2007, doi: 10.1049/.iet-com:20060376.

[24] A. Y. Hassan, "A time diversity scheme with multi-symbol detector for data transmission through flat fading Rayleigh channels," *Phys. Commun.*, vol. 45, Apr. 2021, Art. no. 101277.

[25] A. Y. Hassan, "A frequency-diversity system with diversity encoder and OFDM modulation," *IEEE Access*, vol. 9, pp. 2805–2818, 2021, doi: 10.1109/ACCESS.2020.3047688.

[26] M. Tolga Duman; Ali Ghrayeb, "Fading channels and diversity techniques," in *Coding for MIMO Communication Systems*. Hoboken, NJ, USA: Wiley, 2007, pp. 7–42, doi: 10.1002/.9780470724347.ch2.

[27] *Diversity Techniques for Radio-Relay Systems*, document Rec. ITU-R F.752-1, 1994.

[28] *Key Characteristics for the International Mobile Telecommunications-2000 (IMT 2000) Radio Interfaces*, document ITU-R M.1455-2, 2003.

[29] *Propagation Data and Prediction Methods Required for the Design of Earth-Space Telecommunication System*, document Rec. ITU-R P.618-8, 2003.

[30] *LTE; Evolved Universal Terrestrial Radio Access (E-UTRA); Long Term Evolution (LTE) Physical Layer*, Standard ETSI TS 136 201, V15.3.0, Apr. 2020.

[31] *5G; NR; Physical Layer; General Description*, Standard ETSI TS 138 201 V15.0.0, Sep. 2018.

[32] A. Y. Hassan, "Increasing the symbol rate in QAM system using a new set of orthonormal basics functions," *J. Electr. Syst. Inf. Technol.*, vol. 5, no. 2, pp. 158–174, Sep. 2018, doi: 10.1016/j.jesit.2017.05.007.

[33] S. Verdu, *Multiuser Detection*, 1st ed. Cambridge, U.K.: Cambridge Univ. Press, 1998.

[34] J. G. Proakis, *Digital Communications*. New York, NY, USA: McGraw-Hill, 2001.

[35] M. K. Simon and M. S. Alouini, *Digital Communications over Fading Channels*. New York, NY, USA: Wiley, 2000.

ASHRAF YAHIA HASSAN received the B.Sc. (Hons.) and M.S. degrees in electrical engineering from Benha University, Banha, Egypt, in 2000 and 2004, respectively, and the Ph.D. degree in electronics and electrical communications engineering from Cairo University, Cairo, in 2010.

From 2000 to 2010, he served as a Research and Teaching Assistant at the Electrical Technology Department, Benha Faculty of Engineering. In 2010, he employed as an Assistant Professor in electronics and communication engineering at the Electrical Engineering Department. He worked nine years as a Researcher at the Research and Development Center, Egyptian Telephone Company, from 2000 to 2009. From 2012 to 2015, he worked as a Visiting Assistant Professor at the Faculty of Engineering, Northern Border University, Saudi Arabia. In 2017, he was promoted to an Associate Professor. He was the Head of the Electrical Engineering Department, Benha Faculty of Engineering, Benha University, from 2017 to 2019. Currently, he is the head of a research group working in physical layer researches for new communication standards such as 5G, DVB-S2, and ISDB-S3 standards. His current research interests include detection and estimation theory, digital communication systems, modelling of time-varying channels, interference cancellation techniques, signal processing, coding for high-data-rate wireless and digital communications, and modem design for broadband systems.

AHMED SAMI MOHAMMED received the B.Sc. degree in electronics and communications and the master's degree in electronics and communications from the Benha Faculty of Engineering, Benha University, Egypt, in 2009 and 2015, respectively, where he is currently pursuing the Ph.D. degree with the Electronics and Communications Department.